J Biol Inorg Chem (2014) 19:691–703
DOI 10.1007/s00775-013-1082-5

MINIREVIEW

Comparison of the π-stacking properties of purine versus pyrimidine residues. Some generalizations regarding selectivity

Astrid Sigel · Bert P. Operschall · Helmut Sigel

Received: 9 October 2013 / Accepted: 18 December 2013 / Published online: 25 January 2014
© SBIC 2014

Abstract Aromatic-ring stacking is pronounced among the noncovalent interactions occurring in biosystems and therefore some pertinent features regarding nucleobase residues are summarized. Self-stacking decreases in the series adenine > guanine > hypoxanthine > cytosine ~ uracil. This contrasts with the stability of binary (phen)(N) adducts formed by 1,10-phenanthroline (phen) and a nucleobase residue (N), which is largely independent of the type of purine residue involved, including (N1)H-deprotonated guanine. Furthermore, the association constant for (phen)(A)$^{0/4-}$ is rather independent of the type and charge of the adenine derivative (A) considered, be it adenosine or one of its nucleotides, including adenosine 5′-triphosphate (ATP^{4-}). The same holds for the corresponding adducts of 2,2′-bipyridine (bpy), although owing to the smaller size of the aromatic-ring system of bpy, the (bpy)(A)$^{0/4-}$ adducts are less stable; the same applies correspondingly to the adducts formed with pyrimidines. In accord herewith, [M(bpy)](adenosine)$^{2+}$ adducts (M^{2+} is Co^{2+}, Ni^{2+}, or Cu^{2+}) show the same stability as the (bpy)(A)$^{0/4-}$ ones. The formation of an ionic bridge between $-NH_3^+$ and $-PO_3^{2-}$, as provided by tryptophan [H(Trp)$^{\pm}$] and adenosine 5′-monophosphate (AMP^{2-}), facilitates recognition and stabilizes the indole–purine stack in [H(Trp)](AMP)$^{2-}$. Such indole–purine stacks also occur in nature. Similarly, the formation of a metal ion bridge as occurs, e.g., between Cu^{2+} coordinated to phen and the phosphonate group of 9-[2-(phosphonomethoxy)ethyl]adenine (PMEA^{2-}) dramatically favors the intramolecular stack in Cu(phen)(PMEA). The consequences of such interactions for biosystems are discussed, especially emphasizing that the energies involved in such isomeric equilibria are small, allowing Nature to shift such equilibria easily.

Keywords Aromatic-ring stacking · Binary stacking adducts · Intramolecular stacks · Metal ion complexes · Nucleic acids

1 Introduction

Noncovalent interactions play important roles in modern chemical research [1], including biosystems. Among these interactions aromatic-ring stacking is especially prominent next to hydrogen bonding and hydrophobic and ionic interactions [2–4]. Indeed, such π stacks are crucial for the three-dimensional structures of DNA [2, 5, 6] and RNA [7–9], e.g., in tetraloops and more complicated motifs [10, 11], as well as for ligand recognition [12].

Of course, π–π stacking also occurs in proteins [13], e.g., between the indole side chain of tryptophan and the imidazole residue of histidine [14]. Moreover, stacking interactions are important for charge transfer in proteins [15–17] and also in the double helix of DNA [18–20]. Furthermore, stacking and hydrophobic interactions are of relevance for the formation of protein–nucleic acid adducts [21–23].

This review is dedicated to the memory of Professor Ivano Bertini and his enthusiasm and messianic drive to promote biological inorganic chemistry.

Responsible Editors: Lucia Banci and Claudio Luchinat.

A. Sigel · B. P. Operschall · H. Sigel (✉)
Department of Chemistry,
Inorganic Chemistry,
University of Basel,
Spitalstrasse 51, 4056 Basel, Switzerland
e-mail: helmut.sigel@unibas.ch

It appears that the intensity of the various stacks within DNA affects the charge transport [24, 25]. Indeed, the self-stacking tendency of the various nucleobase residues decreases in the order adenine > guanine > hypoxanthine > cytosine ~ uracil [26–29]; the value for thymine is expected to be at the lower end. In this context we mention the recent proposal that purine–purine base pairs, which are capable of greater stacking interactions (compared with pyrimidines), played an important role in a pre-RNA world [30].

In this review, devoted to the stacking properties of purine and pyrimidine residues, we will concentrate mainly on those of the adenine and cytosine residues by pointing out some new insights. Since self-association occurs for all aromatic-ring systems in various degrees, here only results will be considered where this self-association has been taken into account for both aromatic moieties involved in a stack.

2 Some comments on self-associations

There are various ways to describe and to quantify self-association properties [31]. We will concentrate here on the isodesmic model of indefinite noncooperative self-association as defined by equilibrium 1a and Eq. 1b [26, 32, 33]:

$$(\mathrm{N})_n + \mathrm{N} \rightleftharpoons (\mathrm{N})_{n+1} \quad (1a)$$

$$K_{\mathrm{self}} = [(\mathrm{N})_{n+1}]/([(\mathrm{N})_n][\mathrm{N}]) \quad (1b)$$

This means the monomeric species N forms a dimer with a second monomeric species N, then the dimer plus a further monomeric species N gives rise to a trimer, etc.; the important point is that all equilibrium constants for the various steps are identical.

Figure 1 (top) shows the structures of adenosine (Ado) and cytidine together with the corresponding constants for self-association [26]. As one would expect, the self-association of the purine derivative is more pronounced (by a factor of approximately 10) than that of the pyrimidine derivative. This is in accord with the general expectation that self-association is the more pronounced the larger the aromatic system is, and it agrees further with the already known order given in Sect. 1 for nucleobase residues. These equilibrium constants as well as the other ones given in Fig. 1 were determined by ^{1}H-NMR shift measurements [26, 34, 35].

The effect of the size of the aromatic moiety on the extent of self-association is also nicely borne out from the data shown in the middle part of Fig. 1 [34]. The heteroaromatic amines (Arm) 1,10-phenanthroline (phen) and 2,2′-bipyridine (bpy) are often used in coordination chemistry [36, 37], but also as "indicator" compounds

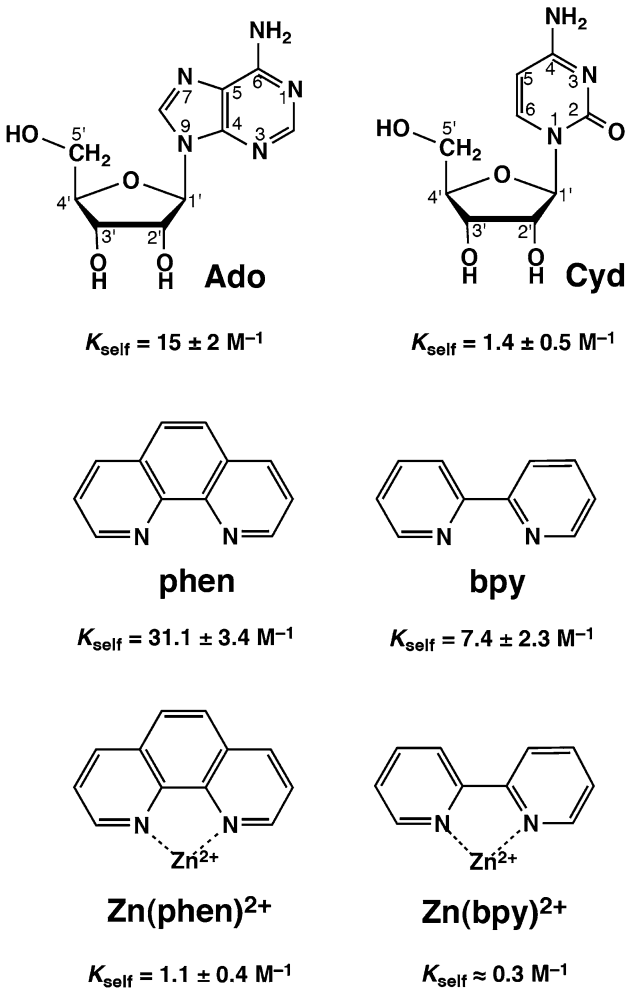

Fig. 1 Chemical structures of the nucleosides adenosine (Ado) and cytidine (Cyd) as well as those of the heteroaromatic nitrogen bases (Arm) 1,10-phenanthroline (phen) and 2,2′-bipyridine (bpy), and their Zn^{2+} complexes, $Zn(phen)^{2+}$ and $Zn(bpy)^{2+}$. Below the structures are given the corresponding self-association constants, K_{self}, as defined by Eq. 1b, together with their error limits (2σ); these constants were measured in D_2O as solvent at 27 °C by ^{1}H-NMR shift experiments ($I = 0.1$ M, $NaNO_3$, except for the Zn^{2+} complexes, where I varied). The constants for the nucleosides, the heteroaromatic amines, and their complexes are taken from [26], [34], and [35], respectively

regarding stack formation, and therefore relatively much information about these two compounds exists (e.g. [4, 38]). We will take advantage of this fact by considering them as well in this review.

As one would expect, coordination of a divalent metal ion such as Zn^{2+} to phen or bpy will strongly reduce the self-association tendency owing to the repulsion of the positive charges of the metal ions which lay within the plane defined by the aromatic moieties. This is nicely borne out from a comparison of the data given in the middle and lower parts of Fig. 1 [35]. Although the self-association is reduced by a factor of approximately 25–30 because of

repulsion, it is not zero and it is still seen that the self-association tendency of $Zn(bpy)^{2+}$ is only approximately one quarter of that of $Zn(phen)^{2+}$. This factor also corresponds with that observed for the self-association of bpy and phen.

To conclude, Fig. 1 confirms that the larger the aromatic moiety is that one considers, the larger is the self-association tendency. The presence of a positive charge (as well as of a negative one [28, 38–40]) reduces the self-association tendency considerably, but it does not completely disappear.

3 Some comments on the stability of binary stacks

The stability of a binary stack formed, e.g., between a heteroaromatic amine (Arm) and a nucleobase residue (N), can be defined according to equilibrium 2a and Eq. 2b:

$$\text{Arm} + \text{N} \rightleftharpoons (\text{Arm})(\text{N}) \quad (2a)$$

$$K^{(\text{N})}_{(\text{Arm})(\text{N})} = [(\text{Arm})(\text{N})]/([\text{Arm}][\text{N}]) \quad (2b)$$

As said before, constants to be determined according to Eq. 2b need to be measured under conditions where either self-association is negligible or it needs to be taken into account [34, 38].

The stability constants for several binary stacks as defined by Eq. 2b are compiled in Table 1 [34, 38, 41, 42]. These data allow many conclusions; the most important ones follow:

1. Entry 1 refers to $(phen)(A)^{0/4-}$ (where A is Ado or one of its nucleotides), for which $K^{(\text{A})}_{(phen)(A)} = 37.4 \pm 2.9\ M^{-1}$ (2σ) is listed. This means the association constant between the aromatic rings of phen and those of the adenine moiety is independent of the residue, be it simply a ribosyl group or a ribosyl 5′-triphosphate. In other words, the stability of the binary stack formed with Ado is within the error limits identical with that of the binary stack formed by adenosine 5′-triphosphate (ATP^{4-}). Of course, the same stability is within the error limits also observed for the $(phen)(AMP)^{2-}$ stacks [41]. Hence, one may conclude that the stability of a binary stack is independent of the charge that one of the partners carries as long as the other partner is neutral and no steric effects are introduced. This is in accord with the other entries listed in Table 1.
2. For $(bpy)(A)^{0/4-}$ (entry 2) the same comments hold as given above for $(phen)(A)^{0/4-}$. However, the stability of the binary $(bpy)(A)^{0/4-}$ stacks is smaller by a factor of about 1/2 than the stability observed for $(phen)(A)^{0/4-}$. This agrees with the expectation because the overlap of a purine system with that of bpy will be smaller than the overlap of a purine system with phen.
3. Replacement of adenine by either an uracil or a cytosine moiety leads to a significant further reduction in stability of the binary stacks as is seen from a comparison of the values in entries 3 and 4 with the value in entry 2. The reduction by a factor of about 1/7 is very pronounced.
4. In accord with the effect of charges mentioned above, $[M(bpy)](Ado)^{2+}$ (entry 5), where M^{2+} is Co^{2+}, Ni^{2+}, or Cu^{2+}, shows the same stability within the error limits as $(bpy)(A)^{0/4-}$ (entry 2). This means the twofold positive charge at bpy due to M^{2+} coordination has no significant effect on the stability of the stack formed with Ado. Of course, with adenosine 5′-monophosphate (AMP^{2-}) this is different [41] because then the two aromatic partners involved in the formation of the stack can be linked by a coordinated metal ion (see Sect. 5).

Table 1 Stability constants of several (Arm)(N) stacks (Eq. 2b), where Arm is a heteroaromatic amine and N is a nucleoside derivative, in aqueous solution as determined by ^{1}H-NMR shift (*entries 1–4*) or UV spectrophotometric (*entry 5*) measurements at a temperature close to 25 °C and *I* close to 0.1 M ($NaNO_3$)

Entry	(Arm)(N)	$K^{(\text{N})}_{(\text{Arm})(\text{N})}$ (M^{-1})	log $K^{(\text{N})}_{(\text{Arm})(\text{N})}$	References
1	$(phen)(A)^{0/4-}$	37.4 ± 2.9[a]	1.57 ± 0.04[a]	–
2	$(bpy)(A)^{0/4-}$	18 ± 8	1.26 ± 0.19	[38]
3	$(bpy)(U)^{0/4-}$	~2.3	~0.36	[38]
4	$(bpy)(C)^{0/4-}$	~2.5[b]	~0.4[b]	–
5	$[M(bpy)](Ado)^{2+}$	18.3 ± 4.5	1.26 ± 0.11	[38, 42]

The NMR measurements were made in D_2O; for details see [38]. The error limits are twice the standard error of the mean value (2σ)

A = adenosine (Ado) or residue; bpy = 2,2′-bipyridine; C = cytidine or residue; M^{2+} = Co^{2+}, Ni^{2+}, or Cu^{2+}; phen = 1,10-phenanthrolin; U = uridine or residue

[a] Average of the values listed in Table 4 in [38] for the adducts (phen)(Ado) [38], $(phen)(2'\text{-AMP})^{2-}$ [41], $(phen)(3'\text{-AMP})^{2-}$ [41], $(phen)(5'\text{-AMP})^{2-}$ [41], and $(phen)(ATP)^{4-}$ [34]

[b] Estimate

4 The favorable effect of an ionic bridge on the formation of a binary stack

Figure 2 shows the structures of the zwitterionic form of tryptophan [$H(Trp^{\pm})$], an amino acid residue often present in proteins and involved in stack formation [13, 14], together with the adenine nucleotide AMP^{2-} [43–45].

Entry 1 in Table 2 gives the stability of the stack formed between the indole residue of Trp^- and the purine-ring system of AMP^{2-}, i.e., for the species $(Trp)(AMP)^{3-}$ [46]. Both partners carry a negative charge at the carboxylate group and the phosphate residue, respectively; however,

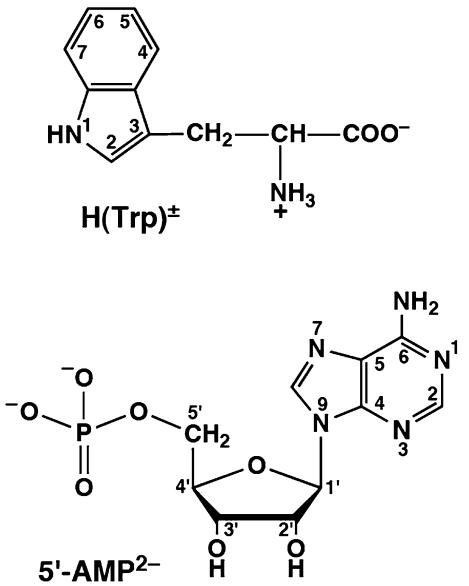

Fig. 2 Chemical structures of the zwitterionic form of tryptophan [$H(Trp)^{\pm}$] and adenosine 5′-monophosphate (5′-AMP^{2-}) (also abbreviated simply as AMP^{2-}). The nucleotide is shown in its dominating anti conformation [6, 43–45]

Table 2 Stability constants (analogous to Eq. 2b) of the adducts formed between Trp^{-} or $H(Trp)^{\pm}$ (=T) and AMP^{2-}, ATP^{4-}, or CMP^{2-} (=N) as determined by ^{1}H-NMR shift measurements in D_2O at 27 °C and $I = 0.1$ M (KNO_3 or $NaNO_3$)

Entry	(T)(N)	$K^{(A)}_{(T)(A)}$ (M^{-1})	References
1	$(Trp)(AMP)^{3-}$	2.24 ± 0.58	[46]
2	$[H(Trp)](AMP)^{2-}$	6.83 ± 1.62	[46]
3	$[H(Trp)](ATP)^{4-}$	6.2 ± 1.2	[47]
4	$(Trp)(CMP)^{3-}$	0.14 ± 0.05	[46]
5	$[H(Trp)](CMP)^{2-}$	0.77 ± 0.42	[46]

The error limits for entries 1–3 are 2σ; those for entries 4 and 5 are estimates

because both charged residues are relatively far away from the aromatic moieties, the charged groups can be orientated such that they are relatively distant from each other and therefore the repulsion is relatively small. However, if one measures the association between AMP^{2-} and tryptophan under conditions (pD = 8.4) where the latter is present in its zwitterionic form $H(Trp)^{\pm}$, the amino group carrying a proton (entry 2), an interaction between the $-NH_3^{+}$ and the $-PO_3^{2-}$ groups results (Fig. 2) [46]. This interaction leads to an ionic bridge (or hydrogen bond) between the indole and adenine residues forming the stack. This bridge enhances the stability of the adduct (entry 2) by a factor of approximately 3 and thus facilitates the recognition between the indole and adenine residues.

Entry 3 in Table 2 gives the stability of the $[H(Trp)](ATP)^{4-}$ adduct [47]. In this case an ionic bridge can be formed as well, although it is not clear, of course, which phosphate unit is actually involved; possibly there are equilibria. However, within the error limits, the stabilities of $[H(Trp)](ATP)^{4-}$ and $[H(Trp)](AMP)^{2-}$ are identical.

Entries 4 and 5 in Table 2 mirror the results discussed for the adenine nucleotides, except that the stabilities of the CMP^{2-} adducts are, as expected, much smaller.

Evidently in the $H(Trp)^{\pm}$ adducts in solution not only a stack with an ionic bridge is present but there are also two "open" isomers: one with only an ionic interaction (ii) and one where only a stack (st) without the ionic bridge occurs [46]. The stability of the latter for the AMP^{2-} adduct in a first approximation is given by entry 1 in Table 2 ($2.24 \pm 0.58\ M^{-1}$; 2σ), whereas the stability for the adduct with the ionic interaction has been estimated as being close to $K_{ii} = 1.0 \pm 0.5\ M^{-1}$ (average of the values given in [46]). These values can now be used to estimate the percentages of the various adducts formed. Clearly, there are three different isomers in equilibrium with each other, which are, if we abbreviate $H(Trp)^{\pm}$ as $H{\cdot}T^{\pm}$ and AMP^{2-} as A^{2-}, the two "open" species $(H{\cdot}T)(A)^{2-}_{st}$ and $(H{\cdot}T)(A)^{2-}_{ii}$, plus the "closed" one $(H{\cdot}T)(A)^{2-}_{cl}$, in which both the ionic and the stacking interactions occur. The measured (exp) stability constant, which quantifies the total (tot) amount of adducts formed, is defined by Eqs. 3a and 3b and it is composed of the (micro) stability constants given in Eq. 3c:

$$K^{(A)}_{(H\cdot T)(A)_{exp}} = \frac{[(H\cdot T)(A)^{2-}_{tot}]}{[(H\cdot T)^{\pm}][(A)^{2-}]} \tag{3a}$$

$$K^{(A)}_{(H\cdot T)(A)_{exp}} = \frac{[(H\cdot T)(A)^{2-}_{st}] + [(H\cdot T)(A)^{2-}_{ii}] + [(H\cdot T)(A)^{2-}_{cl}]}{[(H\cdot T)^{\pm}][(A)^{2-}]} \tag{3b}$$

$$K^{(A)}_{(H\cdot T)(A)_{exp}} = K^{(A)}_{(H\cdot T)(A)_{st}} + K^{(A)}_{(H\cdot T)(A)_{ii}} + K^{(A)}_{(H\cdot T)(A)_{cl}} \tag{3c}$$

Insertion of the (micro) constants mentioned above (see also Table 2) into Eq. 3c leads to Eq. 4, from which the result in Eq. 5 follows:

$$(6.83 \pm 1.62) = (2.24 \pm 0.58) + (1.0 \pm 0.5) + K^{(A)}_{(H\cdot T)(A)_{cl}} \tag{4}$$

$$K^{(A)}_{(H\cdot T)(A)_{cl}} = 3.59 \pm 1.79 \tag{5}$$

Now the right-hand parts of Eqs. 3a and 3b can be set equal, leading to Eqs. 6a and 6b and the molar fractions given in Eq. 7:

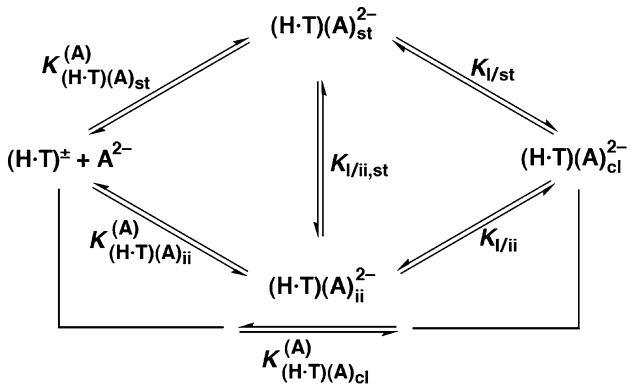

Fig. 3 Summary of the various adducts formed between H(Trp)$^{\pm}$ (=H·T$^{\pm}$) and AMP^{2-} (=A^{2-}) and their corresponding equilibrium constants. For the definition and properties of the various species, see the text in Sect. 4

$$\left[(\mathrm{H{\cdot}T})(\mathrm{A})^{2-}_{\mathrm{tot}}\right] = \left[(\mathrm{H{\cdot}T})(\mathrm{A})^{2-}_{\mathrm{st}}\right] + \left[(\mathrm{H{\cdot}T})(\mathrm{A})^{2-}_{\mathrm{ii}}\right] + \left[(\mathrm{H{\cdot}T})(\mathrm{A})^{2-}_{\mathrm{cl}}\right] \tag{6a}$$

$$(6.83 \pm 1.62) = (2.24 \pm 0.58) + (1.0 \pm 0.5) + (3.59 \pm 1.79) \tag{6b}$$

$$1 = (0.328 \pm 0.114) + (0.146 \pm 0.081) + (0.526 \pm 0.291) \tag{7}$$

Hence, the formation degrees (error 2σ) of the three isomers $(\mathrm{H{\cdot}T})(\mathrm{A})^{2-}_{\mathrm{st}}$, $(\mathrm{H{\cdot}T})(\mathrm{A})^{2-}_{\mathrm{ii}}$, and $(\mathrm{H{\cdot}T})(\mathrm{A})^{2-}_{\mathrm{cl}}$ follow as given in Eq. 8:

$$100\ \% = (33 \pm 11)\ \% + (15 \pm 8)\ \% + (53 \pm 29)\ \% \tag{8}$$

Not surprisingly, the open isomer with an ionic bridge (hydrogen bond), $(\mathrm{H{\cdot}T})(\mathrm{A})^{2-}_{\mathrm{ii}}$, is a minority species (about 15 %), whereas the closed isomer, $(\mathrm{H{\cdot}T})(\mathrm{A})^{2-}_{\mathrm{cl}}$, involving both types of interactions is the dominating one (about 55 %). Moreover, the sum of the species containing an aromatic-ring stack is the overwhelming adduct (nearly 90 %, i.e., 53 + 33 %). Naturally, with the results presented at hand, one may also calculate the intramolecular equilibrium constants (K_{I}) for the transformation of one isomer into another one. The interdependencies between these equilibria are summarized in the equilibrium scheme shown in Fig. 3. The corresponding dimensionless equilibrium constants are approximately $K_{\mathrm{I/st}} = [(\mathrm{H{\cdot}T})(\mathrm{A})^{2-}_{\mathrm{cl}}]/[(\mathrm{H{\cdot}T})(\mathrm{A})^{2-}_{\mathrm{st}}] = 0.526/0.328 \approx 1.60$, $K_{\mathrm{I/ii}} = [(\mathrm{H{\cdot}T})(\mathrm{A})^{2-}_{\mathrm{cl}}]/[(\mathrm{H{\cdot}T})(\mathrm{A})^{2-}_{\mathrm{ii}}] = 0.526/0.146 \approx 3.60$, and $K_{\mathrm{I/ii,st}} = [(\mathrm{H{\cdot}T})(\mathrm{A})^{2-}_{\mathrm{st}}]/[(\mathrm{H{\cdot}T})(\mathrm{A})^{2-}_{\mathrm{ii}}] = 0.328/0.146 \approx 2.25$.

With the above information in mind, it is no surprise to find that protein–nucleic acid interactions in biosystems may occur on the basis of Trp/indole–AMP/adenine stacks. Figure 4 presents such an example [48, 49]. It is of additional interest to see in Fig. 4 that the RNA hairpin is further stabilized by stacks between four consecutive (somewhat twisted) adenine residues; indeed, among all

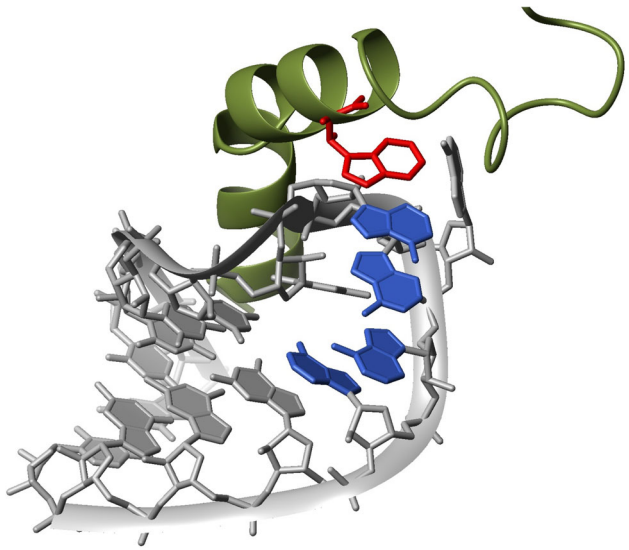

Fig. 4 Stack formation between an indole residue (*red*) of a protein-tryptophan and an adenine–RNA moiety (*blue*) in the N36 peptide-box B RNA complex of bacteriophage Lambda [48]. The figure was prepared with MOLMOL [49] using Protein Data Bank entry 1QFQ

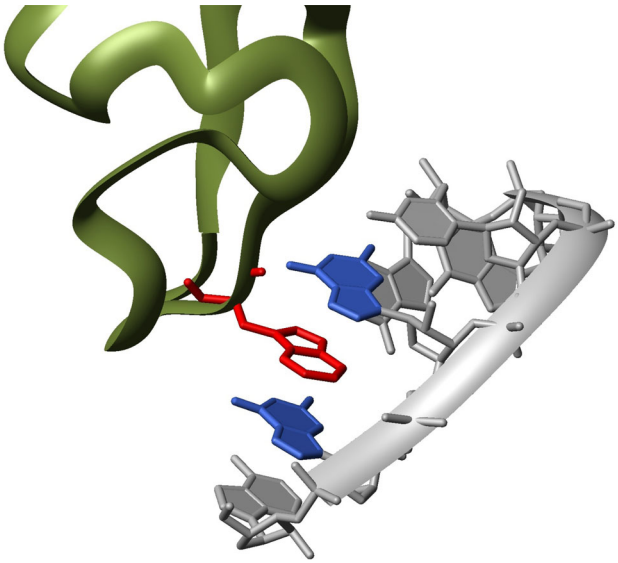

Fig. 5 Stack formation between an indole residue (*red*) of a protein-tryptophan and guanine–RNA moieties (*blue*) in the SR-like protein ZRANB2 and the RNA in its single-stranded RNA-binding domain [52]. The figure was prepared with MOLMOL [49] using the Protein Data Bank entry 3G9Y

nucleobases, self-association is most pronounced for the adenine moiety (see Sect. 1). Such adenine–adenine stacks are also of relevance for the oxidation of oligonucleotides [50]. Combinations of π–π interactions also occur in recognition reactions, e.g., between the tyrosine or phenylalanine residues of a protein and the cytosine or adenine moieties of an RNA, respectively [51].

The self-association of the guanine residue (K_{self}^{Guo} = 8 ± 3 M^{-1}; Eq. 1b [28]) is only about half as pronounced as that of the adenine residue (K_{self}^{Ado} = 15 ± 3 M^{-1}; see Sect. 1 [26–28]), yet the stability of the binary nucleoside stacks involving phen is within the error limits identical; the stability constants according to Eq. 2b [38] are: $K_{(phen)(Ado)}^{Ado}$ = 42 ± 9.5 M^{-1} for (phen)(Ado), 42 ± 5 M^{-1} for (phen)(Guo), and (42 ± 5.5 M^{-1}) for (phen)(Guo − H)$^-$. Hence, it is no surprise to find an intercalated indole residue between two guanine moieties in a zinc finger–RNA adduct (Fig. 5) [52].

Naturally, in the above examples (Figs. 4, 5) stack formation is indirectly facilitated by a suitable organization of the backbones of the macromolecules.

5 A metal ion bridge favors the extent of stacking interactions involving nucleotide analogues

5.1 General considerations on the properties of acyclic nucleoside phosphonates

Provided the two aromatic moieties involved in the formation of a stack also have groups that allow the coordination of a metal ion in a suitable manner, then a bridge between the two partners involved in the stack may be formed. Because relatively comprehensive information exists on phosphonomethoxyethyl derivatives, which contain a nucleobase residue, we have selected 1-[2-(phosphonomethoxy)ethyl]cytosine (PMEC) and 9-[2-(phosphonomethoxy)ethyl]adenine (PMEA) for our comparisons. Both compounds can be considered as acyclic nucleoside phosphonates; they are of interest owing to their potential antiviral activity and therefore they are widely studied [53–55]. Figure 6 shows the structures of the dianions of PMEC and PMEA, which, aside from possible other sites, offer a phosphonate group for metal ion binding. The "aliphatic" chains of the two nucleobases are mimicked by (ethoxymethyl)phosphonate (PME^{2-}) depicted at the top of Fig. 6.

The acyclic nucleoside phosphonates $PMEC^{2-}$ and $PMEA^{2-}$ are of course able to undergo stack formation with the heteroaromatic amines shown in Fig. 1, allowing in addition the formation of a metal ion bridge by coordination of a metal ion to the pyridine-type N sites of heteroaromatic amines and the phosphonate groups of the PME^{2-} derivatives. As examples, the tentative and simplified structures of Cu(phen)(PMEC) and Cu(phen)-(PMEA) containing an intramolecular stack are shown in the lower part of Fig. 6.

The situation is somewhat complicated by the formation of a five-membered chelate formed by the phosphonate-

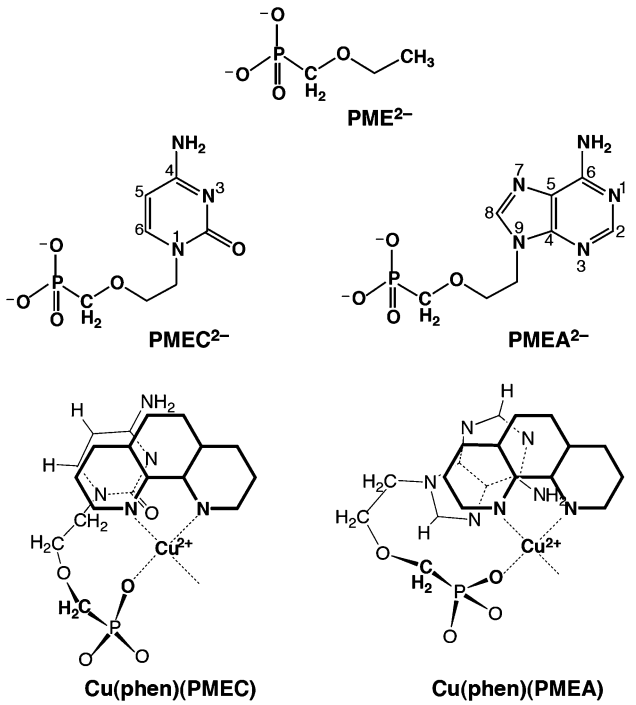

Fig. 6 Chemical structures of the dianions of (phosphonomethoxy)ethane [PME^{2-} = (ethoxymethyl)phosphonate], 1-[2-(phosphonomethoxy)ethyl]cytosine ($PMEC^{2-}$), and 9-[2-(phosphonomethoxy)ethyl]-adenine ($PMEA^{2-}$); these three compounds are abbreviated as PE^{2-}. Also shown are tentative and simplified structures of Cu(phen)(PMEC) and Cu(phen)(PMEA) species with an intramolecular stack. The orientation of the aromatic rings may vary among the stacked species; such a stacked complex in solution should not be considered as being rigid; hence, equilibria are expected between such stacks

coordinated metal ion with the ether oxygen of the aliphatic chain [54, 56, 57]. This gives rise to the intramolecular equilibrium 9, the position of which is quantified by the dimensionless equilibrium constant K_I (Eq. 10):

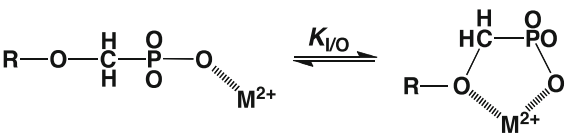

(9)

$$K_{I/O} = [M(PE)_{cl/O}] \Big/ [M(PE)_{op}] \quad (10)$$

(PE^{2-} is PME^{2-}, $PMEC^{2-}$, or $PMEA^{2-}$).

Of course, any metal ion interaction next to the interaction with the phosphonate group must lead to enhanced complex stability [58, 59]. This is nicely seen, e.g., in Fig. 7, where the straight line as defined by the log $K_{Cu(phen)(R-PO_3)}^{Cu(phen)}$ versus $pK_{H(R-PO_3)}^{H}$ plot represents the stability of Cu(phen)(R–PO_3) species. This straight line was determined by using for R–PO_3^{2-} ligands such as ribose 5-phosphate, methylphosphonate, and ethylphosphonate,

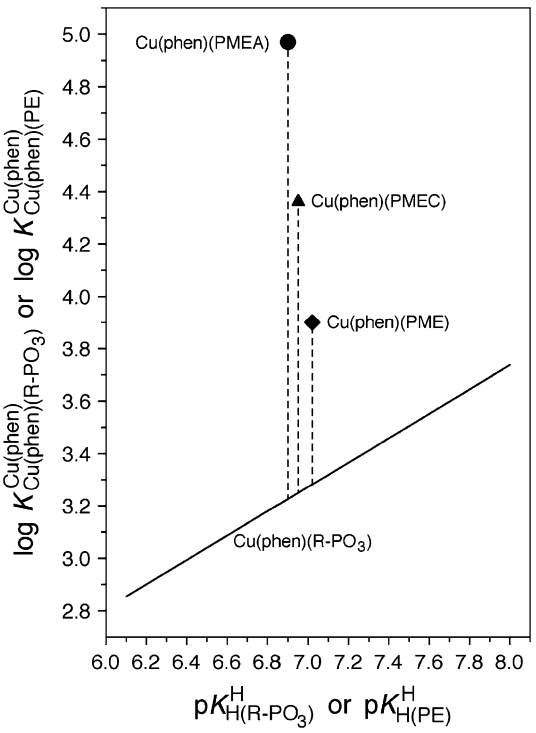

Fig. 7 Evidence for an enhanced stability of ternary Cu(phen)(PE) complexes, where PE^{2-} is PME^{2-} (*diamond*), $PMEC^{2-}$ (*triangle*), or $PMEA^{2-}$ (*circle*), based on the relationship between log $K^{Cu(phen)}_{Cu(phen)(R-PO_3)}$ or log $K^{Cu(phen)}_{Cu(phen)(PE)}$ and $pK^{H}_{H(R-PO_3)}$ or $pK^{H}_{H(PE)}$ in aqueous solution at $I = 0.1$ M ($NaNO_3$) and 25 °C. The data plotted are from [60–62]. The reference line represents the log $K^{Cu(phen)}_{Cu(phen)(R-PO_3)}$ versus $pK^{H}_{H(R-PO_3)}$ relationship for the ternary Cu(phen)(R–PO_3) complexes (Eq. 18); R–PO_3^{2-} symbolizes phosphonates or phosphate monoesters in which the group R is unable to undergo any kind of hydrophobic, stacking, or other type of interaction, i.e., ligands such as D-ribose 5-monophosphate, methanephosphonate, or ethanephosphonate [61, 63]. Hence, the *straight line* represents the situation for ternary complexes without an intramolecular ligand–ligand interaction. The *vertical broken lines* emphasize the stability differences from the reference line; they equal log $\Delta_{Cu/Arm/PE}$ as defined in Eqs. 16a and 16b

that is, ligands which cannot undergo any metal ion interaction aside from interaction with the PO_3^{2-} group [60–62].

In Fig. 7 one sees that the Cu(phen)(PME) complex is more stable than expected according to the basicity of the phosphonate group of PME^{2-} [63]. Hence, equilibrium 9 definitely exists. However, it is further evident from Fig. 7 that the stabilities of the Cu(phen)(PMEC) and Cu(phen)(PMEA) complexes are even higher than the stability of Cu(phen)(PME) [61, 62, 64]. This must mean that in these two complexes containing an acyclic nucleoside phosphonate derivative, next to the five-membered chelate seen in equilibrium 9, a further interaction must occur, namely, stack formation as shown in the lower part of Fig. 6. This stack formation (also proven by other methods [62, 64]) is indicated in the intramolecular equilibrium 11, the position of which is defined by $K_{I/st}$ according to Eq. 12:

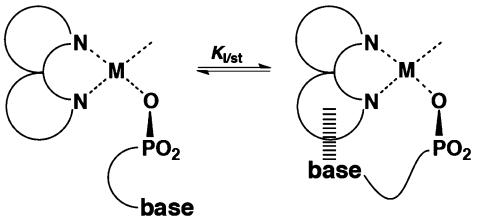

(11)

$$K_{I/st} = [M(Arm)(PE)_{st}]/[M(Arm)(PE)_{op}] \quad (12)$$

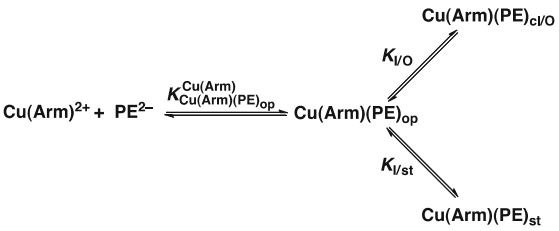

(13)

The situation described in the preceding paragraph can be summarized in the equilibrium scheme 13 from which it follows that $Cu(Arm)(PE)_{op}$ species can form either the five-membered chelate designated as $Cu(Arm)(PE)_{cl/O}$ or the stacked species designated as $Cu(Arm)(PE)_{st}$. The simultaneous formation of the five-membered chelate within the equatorial Cu^{2+} sites and the formation of a stack within the same ternary complex is not possible as concluded previously [61, 65], but stacks with somewhat different orientations of the aromatic rings towards each other may exist. As there is at present no way to distinguish in solution the various conformers/isomers from each other, all stacked ternary species are treated together and designated as $Cu(Arm)(PE)_{st}$, as already done above. Stack formation has not only been established in the indirect manner via stability considerations, as discussed here (Fig. 7), but also directly by spectroscopic methods (for references, see [64]).

5.2 Evaluation of the equilibria involving three isomeric complexes

From the discussion in Sect. 5.1 it follows that there are three isomeric complexes in equilibrium with each other, and this means that for the experimentally measured overall stability constant the following equations hold [57, 61, 65, 66]:

$$K^{Cu(Arm)}_{Cu(Arm)(PE)} = \frac{[Cu(Arm)(PE)]}{[Cu(Arm)^{2+}][PE^{2-}]} \quad (14a)$$

$$K^{\mathrm{Cu(Arm)}}_{\mathrm{Cu(Arm)(PE)}} = \frac{[\mathrm{Cu(Arm)(PE)_{op}}] + [\mathrm{Cu(Arm)(PE)_{cl/O}}] + [\mathrm{Cu(Arm)(PE)_{st}}]}{[\mathrm{Cu(Arm)^{2+}}][\mathrm{PE^{2-}}]} \quad (14b)$$

$$K^{\mathrm{Cu(Arm)}}_{\mathrm{Cu(Arm)(PE)}} = K^{\mathrm{Cu(Arm)}}_{\mathrm{Cu(Arm)(PE)_{op}}}(1 + K_{\mathrm{I/O}} + K_{\mathrm{I/st}}) \quad (14c)$$

Of course, the stability of the open species is defined by Eq. 15 as follows from the equilibrium scheme 13.

$$K^{\mathrm{Cu(Arm)}}_{\mathrm{Cu(Arm)(PE)_{op}}} = \frac{[\mathrm{Cu(Arm)(PE)_{op}}]}{[\mathrm{Cu(Arm)^{2+}}][\mathrm{PE^{2-}}]} \quad (15)$$

Furthermore from Fig. 7 it follows that the stability enhancement log $\Delta_{\mathrm{Cu/Arm/PE}}$ is defined by Eqs. 16a and 16b:

$$\log \Delta_{\mathrm{Cu/Arm/PE}} = \log K^{\mathrm{Cu(Arm)}}_{\mathrm{Cu(Arm)(PE)}} - \log K^{\mathrm{Cu(Arm)}}_{\mathrm{Cu(Arm)(PE)_{op}}} \quad (16a)$$

$$\log \Delta_{\mathrm{Cu/Arm/PE}} = \log K^{\mathrm{Cu(Arm)}}_{\mathrm{Cu(Arm)(PE)_{exptl}}} - \log K^{\mathrm{Cu(Arm)}}_{\mathrm{Cu(Arm)(PE)_{calcd}}} \quad (16b)$$

The two terms which appear on the right hand side in Eqs. 16a and 16b are analogous. The first one is the measured constant and the second one, which represents the stability of the open isomer (Eq. 15), can be calculated with the $\mathrm{p}K^{\mathrm{H}}_{\mathrm{H(R-PO_3)}}$ value of $\mathrm{H(PE)^-}$ and the straight line Eqs. 17 and 18 for the Cu(bpy)(R–PO_3) and Cu(phen)(R–PO_3) systems, respectively [59, 61]:

$$\log K^{\mathrm{Cu(bpy)}}_{\mathrm{Cu(bpy)(R-PO_3)}} = 0.465 \times \mathrm{p}K^{\mathrm{H}}_{\mathrm{H(R-PO_3)}} + 0.009 \quad (17)$$

$$\log K^{\mathrm{Cu(phen)}}_{\mathrm{Cu(phen)(R-PO_3)}} = 0.465 \times \mathrm{p}K^{\mathrm{H}}_{\mathrm{H(R-PO_3)}} + 0.018 \quad (18)$$

The total stability enhancement according to Eqs. 16a and 16b encompasses, of course, both the formation of the stack (equilibrium 11) and the five-membered chelate involving the ether oxygen (equilibrium 9). Therefore, an overall or total intramolecular equilibrium constant, i.e., $K_{\mathrm{I/tot}}$, can be defined according to Eqs. 19a, 19b, 19c, and 19d:

$$K_{\mathrm{I/tot}} = \frac{K^{\mathrm{Cu(Arm)}}_{\mathrm{Cu(Arm)(PE)}}}{K^{\mathrm{Cu(Arm)}}_{\mathrm{Cu(Arm)(PE)_{op}}}} - 1 = \frac{[\mathrm{Cu(Arm)(PE)_{int/tot}}]}{[\mathrm{Cu(Arm)(PE)_{op}}]} \quad (19a)$$

$$K_{\mathrm{I/tot}} = \frac{[\mathrm{Cu(Arm)(PE)_{cl/O}}] + [\mathrm{Cu(Arm)(PE)_{st}}]}{[\mathrm{Cu(Arm)(PE)_{op}}]} \quad (19b)$$

$$K_{\mathrm{I/tot}} = K_{\mathrm{I/O}} + K_{\mathrm{I/st}} \quad (19c)$$

$$K_{\mathrm{I/tot}} = 10^{\log \Delta_{\mathrm{Cu/Arm/PE}}} - 1 \quad (19d)$$

The values for the equilibrium constants which appear on the right-hand side of Eqs. 16a and 16b are found in the literature [61–63]. For the present, it is only important to note that log $\Delta_{\mathrm{Cu/Arm/PE}}$ corresponds to the vertical distances seen in Fig. 7 between the measured data point of a given complex and the intercept with the straight line representing the stability of the open complex. These log $\Delta_{\mathrm{Cu/Arm/PE}}$ values are listed in the second column in Table 3. Application of Eqs. 19a, 19b, 19c, and 19d to these data provides the values for $K_{\mathrm{I/tot}}$ which are given in column 3. Of course, once $K_{\mathrm{I/tot}}$ is known, one may calculate according to Eq. 20 the total percentage of all species with an intramolecular interaction (Table 3, column 4):

$$\%\ \mathrm{Cu(Arm)(PE)_{int/tot}} = 100 \times K_{\mathrm{I/tot}}/(1 + K_{\mathrm{I/tot}}) \quad (20)$$

At this point two important conclusions may be drawn from the results assembled in Table 3: (1) The first two entries which refer to the Cu(Arm)(PME) complexes describe the situation according to equilibrium 9, i.e., $K_{\mathrm{I/tot}} = K_{\mathrm{I/O}}$ and % $\mathrm{Cu(Arm)(PME)_{int/tot}}$ = % $\mathrm{Cu(Arm)(PME)_{cl/O}}$, and of course, the same $K_{\mathrm{I/O}}$ values are expected to hold for the other entries in rows 3–6 in Table 3. (2) Because column 4 in Table 3 provides the total formation degree of all the species which contain an intramolecular interaction, it follows that % $\mathrm{Cu(Arm)(PE)_{op}}$ = 100 % – % $\mathrm{Cu(Arm)(PE)_{int/tot}}$.

On the basis of the above conclusions, Table 4 contains in the second column the calculated values for % $\mathrm{Cu(Arm)(PE)_{op}}$. Because $K_{\mathrm{I/tot}}$ is known as is $K_{\mathrm{I/O}}$, from Eq. 19c $K_{\mathrm{I/st}}$ can be calculated for the Cu(Arm)-(PMEC) and Cu(Arm)(PMEA) systems. These intramolecular equilibrium constants, $K_{\mathrm{I/st}}$, are listed in column 4 in Table 4. Combination of % $\mathrm{Cu(Arm)(PE)_{op}}$ with $K_{\mathrm{I/O}}$ and $K_{\mathrm{I/st}}$ (see Eqs. 10, 12) provides the results listed in columns 5 and 6 in Table 4. That is, for the Cu(Arm)(PMEC) and Cu(Arm)(PMEA) systems, the percentages of all three isomers which occur in the equilibrium scheme 13 are known.

5.3 Some conclusions about the properties of the Cu(Arm)(PE) complexes

Several conclusions are possible from the results assembled in Table 4:

1. Formation of the ternary complexes with an intramolecular stack occurs on account of the isomers containing the five-membered chelate involving the ether oxygen.
2. The percentage of $\mathrm{Cu(Arm)(PMEC)_{st}}$ does not significantly differ for the complexes containing either bpy or phen; it is close to 65 %. This is understandable because the overlap of a pyrimidine residue with bpy or phen will not differ much.
3. This is different for the systems containing PMEA. Here the stability of the intramolecular stack is higher by a factor of about 2 for the Cu(phen)(PMEA) species compared with that of Cu(bpy)(PMEA) as follows from the $K_{\mathrm{I/st}}$ values (column 4).

Table 3 Stability enhancements, log $\Delta_{Cu/Arm/PE}$ (Eqs. 16a, 16b), and formation degrees, % $Cu(Arm)(PE)_{int/tot}$ (Eq. 20), of the sum (tot) of all species with an intramolecular (int) interaction in several Cu(Arm)(PE) complexes (Eqs. 19a, 19b) as determined in aqueous solution at 25 °C and $I = 0.1$ M ($NaNO_3$)

Cu(Arm)(PE)[a]	log $\Delta_{Cu/Arm/PE}$	$K_{I/tot}$	% $Cu(Arm)(PE)_{int/tot}$	References
Cu(bpy)(PME)	0.59 ± 0.08	2.89 ± 0.68[b]	74 ± 5[b]	[61, 63]
Cu(phen)(PME)	0.62 ± 0.07	3.17 ± 0.69[b]	76 ± 4[b]	[61, 63]
Cu(bpy)(PMEC)	1.02 ± 0.09	9.47 ± 2.22	90.45 ± 2.03	[62]
Cu(phen)(PMEC)	1.11 ± 0.08	11.88 ± 2.32	92.24 ± 1.40	[62]
Cu(bpy)(PMEA)	1.48 ± 0.07	29.20 ± 4.87	96.69 ± 0.53	[61]
Cu(phen)(PMEA)	1.74 ± 0.07	53.95 ± 8.86	98.18 ± 0.29	[61]

The data were abstracted from Table 3 in [62]. The error limits are 3σ

[a] For the structures of the PE^{2-} ligands, see Fig. 6

[b] For the Cu(Arm)(PME) systems, $K_{I/tot} = K_{I/O}$ (Eqs. 10, 19c) holds

Table 4 Formation degrees of the three differently structured Cu(Arm)(PE) isomers as they appear in the equilibrium scheme 13 and as present in aqueous solution at 25 °C and $I = 0.1$ M ($NaNO_3$)

Cu(Arm)(PE)[a]	% $Cu(Arm)(PE)_{op}$	$K_{I/O}$	$K_{I/st}$	% $Cu(Arm)(PE)_{cl/O}$	% $Cu(Arm)(PE)_{st}$
Cu(bpy)(PME)	26 ± 5	2.89 ± 0.68	–	74 ± 5	–
Cu(phen)(PME)	24 ± 4	3.17 ± 0.69	–	76 ± 4	–
Cu(bpy)(PMEC)	9.55 ± 2.03	2.89 ± 0.68	6.58 ± 2.32	28 ± 9	62 ± 9
Cu(phen)(PMEC)	7.76 ± 1.40	3.17 ± 0.69	8.71 ± 2.42	25 ± 7	67 ± 7
Cu(bpy)(PMEA)	3.31 ± 0.53	2.89 ± 0.68	26.31 ± 4.92	10 ± 3	87 ± 3
Cu(phen)(PMEA)	1.82 ± 0.29	3.17 ± 0.69	50.78 ± 8.89	6 ± 2	92 ± 2

The data were abstracted from Table 4 in [62] (for details regarding the PME, PMEC, and PMEA systems see also [63], [62], and [61], respectively). The error limits are 3σ

[a] For the structures of the PE^{2-} ligands, see Fig. 6

4. Of course, as expected, the formation degree of the stacked ternary species containing $PMEA^{2-}$ is much higher than of those containing $PMEC^{2-}$ (see the results in columns 4 and 6).

At this point it is interesting to compare the stacking properties in the ternary Cu(Arm)(L) complexes, where L represents either an acyclic nucleoside phosphonate or one of its parents, i.e., a nucleoside 5′-monophosphate. The corresponding structures are shown in Fig. 8 [39, 67–71].

In entries 1 and 2 in Table 5 the relevant data from Table 4 are repeated. Entries 3 and 4 contain the results for the Cu(Arm)(NMP) systems as taken from the literature [41, 72]. Naturally, in these latter instances, no five-membered chelates according to the equilibrium 9 can be formed, but intramolecular stacking interactions are possible, of course. It is now interesting to see that stack formation is less pronounced in the complexes containing $NMP^{2-} = CMP^{2-}$ or AMP^{2-} than in those containing $PE^{2-} = PMEC^{2-}$ or $PMEA^{2-}$.

The latter point is especially clearly seen from the intramolecular equilibrium constants $K_{I/st}$, which quantify the stability of the intramolecular stacks (Table 5, column

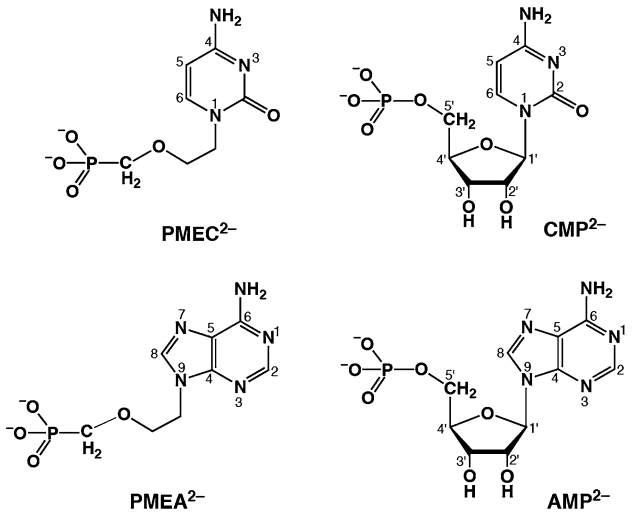

Fig. 8 Comparison of the chemical structures of the acyclic nucleoside phosphonates $PMEC^{2-}$ and $PMEA^{2-}$ and their corresponding parent nucleotides cytidine 5′-monophosphate (CMP^{2-}) and adenosine 5′-monophosphate (AMP^{2-}), respectively. Both nucleotides are shown in their dominating *anti* conformation [39, 44, 67–69]. The orientation of $PMEA^{2-}$ (as shown) in solution [70] (this holds also for the solid state [71]) resembles the *anti* conformation of AMP^{2-} [44, 45]

Table 5 Comparison of the formation degrees of the stacked isomers (Fig. 3, bottom) in the ternary $PMEC^{2-}$ and $PMEA^{2-}$ complexes with those containing the parent nucleotides CMP^{2-} and AMP^{2-} (NMP^{2-}; see Fig. 8)

Entry	Cu(Arm)(PE/NMP)	% Cu(Arm)(PE/NMP)$_{op}$	% Cu(Arm)(PE/NMP)$_{cl/O}$	$K_{I/st}$	% Cu(Arm)(PE/NMP)$_{st}$	References[a]
1a	Cu(Bpy)(PMEC)	9.55 ± 2.03	28 ± 9	6.58 ± 2.32	62 ± 9	[62]
1b	Cu(Phen)(PMEC)	7.76 ± 1.40	25 ± 7	8.71 ± 2.42	67 ± 7	[62]
2a	Cu(Bpy)(PMEA)	3.31 ± 0.53	10 ± 3	26.31 ± 4.92	87 ± 3	[61]
2b	Cu(Phen)(PMEA)	1.82 ± 0.29	6 ± 2	50.78 ± 8.89	92 ± 2	[61]
3a	Cu(Bpy)(CMP)	49 ± 9	–	1.04 ± 0.38[b]	51 ± 9	[72]
3b	Cu(Phen)(CMP)	38 ± 6	–	1.63 ± 0.44[b]	62 ± 6	[72]
4a	Cu(Bpy)(AMP)	19 ± 4	–	4.37 ± 1.02[b]	81 ± 4	[41]
4b	Cu(Phen)(AMP)	10 ± 2	–	8.77 ± 1.81[b]	90 ± 2	[41]

The formation degrees hold for aqueous solutions at 25 °C and $I = 0.1$ M ($NaNO_3$) (error limits 3σ)

[a] See also Table 4 in [62]

[b] For the Cu(Arm)(NMP) systems, $K_{I/tot} = K_{I/st}$ (Eqs. 12, 19c) holds

5). Indeed, the intramolecular stacks in the Cu(Arm)(NMP) complexes are a factor of about 1/6 less stable than those of the Cu(Arm)(PE) species. What is the reason for this somewhat surprising result? A comparison of the structures shown in Fig. 8 reveals that the ribose ring limits the flexibility in the Cu(Arm)(NMP) complexes considerably in comparison with that of the Cu(Arm)(PMEC) and Cu(Arm)(PMEA) species. This increased flexibility allows a more strain-free formation of the intramolecular stacks and thus leads to larger formation degrees.

6 A somewhat speculative application of part of the results to polymerases

First it is necessary to emphasize that to achieve the reactive state of a triphosphate chain, two metal ions or at least two positively charged units including, e.g., $-NH_3^+$, are needed [73, 74]. We will concentrate here on the involvement of two divalent metal ions, and this is summarized in Fig. 9 [74–85]. An M(α,β)–M(γ) coordination mode at the triphosphate chain leads to the transfer of a phosphoryl group (kinases) [74, 75, 86], whereas an M(α)–M(β,γ) binding mode of the two metal ions leads to the transfer of a nucleotidyl unit as occurs in nucleic acid polymerases [74, 76, 79, 84]. In both instances a diphosphate unit could also be transferred, but this is not of relevance in the present context.

At this point it is important to recall that the antiviral properties of acyclic nucleoside phosphonates [54] are achieved by a twofold phosphorylation [87, 88] within the cell giving rise, e.g., to a $PMEApp^{4-}$ species, which is an analogue of $(d)ATP^{4-}$. Evidently, if the $PMEApp^{4-}$ species is used as a substrate and incorporated by the polymerase into the growing nucleic acid chain [89, 90], the chain will be terminated because there is no (C3′)OH group allowing the further growth of the nucleic acid chain [91, 92]. This polymerase reaction is shown in a simplified manner in the lower part of Fig. 9. A comparison between the properties of $M_2(PMEApp)$ and $M_2(dATP)$ reveals why $PMEApp^{4-}$ is a better substrate [54, 82, 83, 93] than $(d)ATP^{4-}$: (1) The M(α) coordination is clearly favored owing to the presence of the ether oxygen, giving rise to a five-membered chelate (Fig. 9, bottom) [65]. (2) The electron density at P_α is higher in the phosphonate (and also the phosphonate basicity) compared with the situation in phosphate [94, 95], thus facilitating the nucleophilic attack. These two properties favoring the M(α)–M(β,γ) coordination pattern make $PMEApp^{4-}$ a better substrate than $dATP^{4-}$ [54, 83].

With the above information in mind, one may ask now why PMEA is an excellent antiviral drug whereas PMEC is not. The speculative answer is that $PMEApp^{4-}$ is well placed in the active-site cavity of the polymerase owing to its more intense stacking properties compared with $PMECpp^{4-}$. Clearly, more work is needed to substantiate the explanation given.

7 General conclusions

The observation that pyridyl and pyrimidine residues have a smaller stacking tendency than larger aromatic moieties such as phen or purine moieties is no surprise. However, the observation that in a binary stack composed of two different aromatic systems one may carry either a positive or a negative charge without a significant alteration of the stability of the binary stack as long as the other partner is neutral, that is, does not also carry a charge, is an important insight and is relevant for biological systems (Sect. 3). For

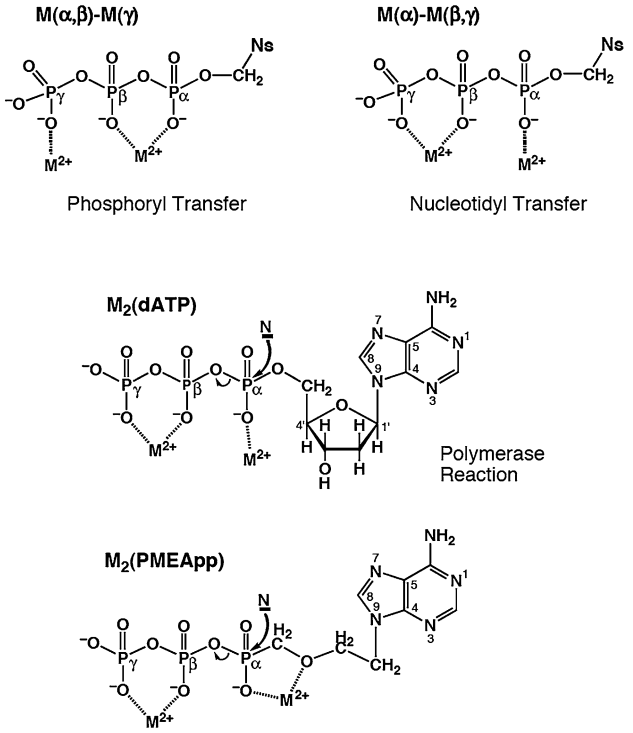

Fig. 9 At the *top* two simplified structures of M_2(NTP) complexes [NTP^{4-} is (2′-deoxy)nucleoside 5′-triphosphate] are shown: one with an M(α,β)-M(γ) coordination mode (*left*) relevant for transphosphorylations (kinases), and one with an M(α)–M(β,γ)-type mode (*right*) relevant for the transfer of a nucleotidyl unit as catalyzed by polymerases. This latter binding mode needs to be enforced by the enzyme, i.e., both metal ions are anchored [74, 75] to amino acid side chains, often carboxylate groups of aspartate or glutamate units of the enzyme [76–81] (CH_2–Ns is a nucleoside residue). Of course, one may think of situations where, e.g., M^{2+} at the β and γ groups is replaced by (a) monovalent metal ion(s) and/or (an) ammonium residue(s) [73, 74]. The simplified structures in the *lower* part of the figure represent the M_2(dATP) and M_2(PMEApp) intermediates ready for the attack of a nucleophile (N) and on their way to the transition state in nucleic acid polymerases [74, 82, 83]. Both metal ions (often Mg^{2+}) [78, 80, 84] need to be anchored to amino acid side chains of the enzyme (see above). The nucleophile N (a 3′-OH group) may in addition interact with M^{2+} at P_α and the adenine moiety may be replaced by any other nucleobase residue. The M(α)–M(β,γ)-binding mode, which is crucial for the polymerase reaction, is favored in M_2(PMEApp) owing to the formation of the five-membered chelate with the ether oxygen of the aliphatic chain [54, 83]

example, a metal ion coordinated at N7 of a purine unit will not significantly affect the stacking properties of this same purine residue. It may be emphasized again in this context that the stabilities of the (phen)(Ado), (phen)(guanosine), and (phen)(guanosine – H*N1*)$^-$ binary stacks are within the error limits identical [38] (see also Sect. 4).

That the formation of a bridge between the two partners of a binary stack will significantly enhance the formation degree of the stack, and thus facilitate recognition between the two partners, has become clear from the results described in Sects. 4 and 5. However, this can be further

Table 6 Interrelation between the stability enhancement log $\Delta_{M/A/B}$ (Eqs. 16a, 16b), the intramolecular equilibrium constant K_I (Eqs. 19a, 19b, 19c, 19d), the percentage of the "closed" species with an intramolecular interaction (II), % $M(A)(B)_{II}$ (Eq. 20), and the change in free energy ΔG^0 at 25 °C

log $\Delta_{M/A/B}$	K_I	% $M(A)(B)_{II}$	ΔG^0 (kJ mol^{-1})
0.05	0.12	10.9	–0.29
0.1	0.26	20.6	–0.57
0.2	0.58	37	–1.14
0.3	1.0	50	–1.71
0.5	2.2	68	–2.86
0.7	4.0	80	–4.00
1.0	9.0	90	–5.71
1.5	30.6	97	–8.57
2.0	99	99	–11.4
3.0	999	99.9	–17.1

emphasized by the following comparison, which refers to 10^{-3} M solutions of the reactants at a pH of approximately 7 (25 °C; $I = 0.1$ M, $NaNO_3$) [34, 38]: (1) In a mixture of phen and ATP^{4-} under the given conditions and in aqueous solution, 3.5 % of the reactants exist as binary (phen)-$(ATP)^{4-}_{st}$ stacks. (2) Under exactly the same conditions but in the presence of Cu^{2+}, 90 % of the reactants are now present as Cu(phen)$(ATP)^{2-}_{st}$. This means the metal ion bridge promotes the formation of the stack by a factor of about 25. In mixed solvents, such as water containing 50 % 1,4-dioxane, the promotion of the stack may even become considerably larger because the organic solvent molecules solvate hydrophobically the individual stacking partners to a certain extent, which inhibits the formation of the binary stacks, whereas this inhibition is considerably less pronounced in the ternary M^{2+} complexes because the M^{2+} ions attract water molecules, thus inhibiting the hydrophobic solvation of the aromatic partners.

At this point it seems helpful to relate the stability enhancements as observed for intramolecular interactions in mixed ligand complexes to the free energies involved in a general manner. The contribution of isomers with an intramolecular interaction to the change in free energy for complex formation is given by $\Delta G^0 = -RT \ln \Delta_{M/A/B}$ [58]. This means for 25 °C it holds $\Delta G^0_{25°C} = -5.71 \times \log \Delta_{M/A/B}$ [59]. On this basis, the data assembled in Table 6 were calculated.

Evidently, a small stability enhancement of log $\Delta_{M/A/B} = 0.1$, valid for any mixed ligand M(A)(B) complex containing ligands A and B, means a formation degree of about 20 % for the species with an intramolecular interaction, for example, a stack. But this corresponds energywise to a change of only $\Delta G^0 = -0.57$ kJ mol^{-1}. The stability enhancement of log $\Delta_{M/A/B} = 0.3$ means that the "closed" species reaches a formation degree of 50 %, but the

change in free energy of -1.71 kJ mol^{-1} is still relatively small. Matters become "costly" only for high formation degrees. For example, a formation degree of an intramolecular interaction of 90 % corresponds to a stability enhancement of 1 log unit and ΔG^0 of -5.71 kJ mol^{-1}.

Of course, the same interrelations between changes in free energy and intramolecular chelate formation also hold for binary complexes of the kind indicated in equilibrium 9. For example, an isolated hydroxyl group, such as in ethanol, is a poor ligand. However, if connected with a suitable primary binding site, such as an acetate or pyridine group as is the case in hydroxyacetate or *o*-(hydroxymethyl)pyridine, respectively, the hydroxyl group transfers into an excellent ligating site [96], an observation of relevance also for ribozymes/nucleic acids.

To conclude, considering the results described in this review, it is clear that the correct structure of a substrate for an enzymatic reaction can be obtained without large changes in free energy. Or, to say it differently, subtle conformational changes may have dramatic effects on "recognition" and the reactivity of a system.

Acknowledgments The support of our work by the Department of Chemistry of the University of Basel is gratefully acknowledged, as is the help in the preparation of Figs. 3 and 4 by Joachim Schnabl and Roland K.O. Sigel from the University of Zurich.

References

1. Barin G, Coskun A, Fouda MMG, Stoddart JF (2012) ChemPlusChem 77:159–185
2. Gahlon HL, Sturla SJ (2013) Chem Eur J 19:11062–11067
3. Yamauchi O, Odani A, Takani M (2002) J Chem Soc Dalton Trans 3411–3421
4. Yamauchi O, Odani A, Masuda H, Sigel H (1996) Met Ions Biol Syst 32:207–270
5. Sigel A, Sigel H, Sigel RKO (eds) (2012) Met Ions Life Sci 10 (Interplay between metal ions and nucleic acids):1–353
6. Saenger W (1984) Principles of nucleic acid structure. Springer, New York, pp 1–556
7. Sigel A, Sigel H, Sigel RKO (eds) (2011) Met Ions Life Sci 9 (Structural and catalytic roles of metal ions in RNA):1–391
8. Sigel RKO, Pyle AM (2007) Chem Rev 107:97–113
9. Erat MC, Zerbe O, Fox T, Sigel RKO (2007) ChemBioChem 8:306–314
10. Donghi D, Pechlaner M, Finazzo C, Knobloch B, Sigel RKO (2013) Nucleic Acids Res 41:2489–2504
11. Butcher SE, Pyle AM (2011) Acc Chem Res 44:1302–1311
12. Phongtongpasuk S, Paulus S, Schnabl J, Sigel RKO, Spingler B, Hannon MJ, Freisinger E (2013) Angew Chem Int Ed 52:11513–11516
13. Bertini I, Sigel A, Sigel H (eds) (2001) Handbook on metalloproteins. Dekker, New York, pp 1–1182
14. Yang CM, Zhang J (2010) Chem Eur J 16:10854–10865
15. Constable EC, Housecroft CE, Creus M, Gademann K, Giese B, Ward TR, Woggon W-D, Chougnet A (2010) Chimia 64:846–854
16. Lee JC, Kim JE, Pletneva EV, Faraone-Mennella J, Gray HB, Winkler JR (2006) Met Ions Life Sci 1:9–60
17. Sigel H, Sigel A (eds) (1991) Met Ions Biol Syst 27 (Electron transfer reactions in metalloproteins):1–537
18. Slinker JD, Muren NB, Renfrew SE, Barton JK (2011) Nat Chem 3:228–233
19. Pratviel G (2012) Met Ions Life Sci 10:201–216
20. Kawai K, Majima T, Maruyama A (2013) ChemBioChem 14:1430–1433
21. Leavens FMV, Churchill CDM, Wang S, Wetmore SD (2011) J Phys Chem B 115:10990–11003
22. Zambelli B, Musiani F, Ciurli S (2012) Met Ions Life Sci 10:135–170
23. Copeland KL, Pellock SJ, Cox JR, Cafiero ML, Tschumper GS (2013) J Phys Chem B 117:14001–14008
24. Kawai K, Kodera H, Osakada Y, Majima T (2009) Nat Chem 1:156–159
25. Genereux JC, Barton JK (2009) Nat Chem 1:106–107
26. Scheller KH, Hofstetter F, Mitchell PR, Prijs B, Sigel H (1981) J Am Chem Soc 103:247–260
27. Scheller KH, Sigel H (1983) J Am Chem Soc 105:5891–5900
28. Corfù NA, Tribolet R, Sigel H (1990) Eur J Biochem 191:721–735
29. Corfù NA, Sigel H (1991) Eur J Biochem 199:659–669
30. Kuruvilla E, Schuster GB, Hud NV (2013) ChemBioChem 14:45–48
31. Martin RB (1996) Chem Rev 96:3043–3064
32. Mitchell PR, Sigel H (1978) Eur J Biochem 88:149–154
33. Neurohr KJ, Mantsch HH (1979) Can J Chem 57:1986–1994
34. Tribolet R, Malini-Balakrishnan R, Sigel H (1985) J Chem Soc Dalton Trans 2291–2303
35. Mitchell PR (1980) J Chem Soc Dalton Trans 1079–1086
36. von Grebe P, Suntharalingam K, Vilar R, Sanz Miguel PJ, Herres-Pawlis S, Lippert B (2013) Chem Eur J 19:11429–11438
37. Ye R-R, Ke Z-F, Tan C-P, He L, Ji L-N, Mao Z-W (2013) Chem Eur J 19:10160–10169
38. Corfù NA, Sigel A, Operschall BP, Sigel H (2011) J Indian Chem Soc 88:1093–1115 (Sir A. Prafulla Chandra Ray commemoration issue)
39. Tribolet R, Sigel H (1987) Biophys Chem 27:119–130
40. Tribolet R, Sigel H (1988) Eur J Biochem 170:617–626
41. Massoud SS, Tribolet R, Sigel H (1990) Eur J Biochem 187:387–393
42. Chaudhuri P, Sigel H (1977) J Am Chem Soc 99:3142–3150
43. Martin RB, Mariam YH (1979) Met Ions Biol Syst 8:57–124
44. Tribolet R, Sigel H (1987) Eur J Biochem 163:353–363
45. Aoki K (1996) Met Ions Biol Syst 32:91–134
46. Orenberg JB, Fischer BE, Sigel H (1980) J Inorg Nucl Chem 42:785–792
47. Mitchell PR, Prijs B, Sigel H (1979) Helv Chim Acta 62:1723–1735
48. Schaerpf M, Sticht H, Schweimer K, Boehm M, Hoffmann S, Roesch P (2000) Eur J Biochem 267:2397–2408
49. Koradi R, Billeter M, Wüthrich K (1996) J Mol Graph 14:29–32
50. Capobianco A, Caruso T, Celentano M, D'Ursi AM, Scrima M, Peluso A (2013) J Phys Chem B 117:8947–8953
51. Blakeley BD, Shattuck J, Coates MB, Tran E, Laird-Offringa IA, McNaughton BR (2013) Biochemistry 52:4745–4747
52. Loughlin FE, Mansfield RE, Vaz PM, McGrath AP, Setiyaputra S, Gamsjaeger R, Chen ES, Morris BJ, Guss JM, Mackay JP (2009) Proc Natl Acad Sci USA 106:5581–5586
53. Holý A (2003) Curr Pharm Des 9:2567–2592
54. Sigel H (2004) Chem Soc Rev 33:191–200
55. Tichy T, Andrei G, Dračínský M, Holý A, Balzarini J, Snoeck R, Krečmerová M (2011) Bioorg Med Chem 19:3527–3539

56. Fernández-Botello A, Holý A, Moreno V, Operschall BP, Sigel H (2009) Inorg Chim Acta 362:799-810 (issue in honor of B. Lippert)
57. Fernández-Botello A, Griesser R, Holý A, Moreno V, Sigel H (2005) Inorg Chem 44:5104–5117
58. Martin RB, Sigel H (1988) Comments Inorg Chem 6:285–314
59. Sigel H, Kapinos LE (2000) Coord Chem Rev 200–202:563–594
60. Sigel H, Chen D, Corfù NA, Gregáň F, Holý A, Strašák M (1992) Helv Chim Acta 75:2634–2656
61. Chen D, Bastian M, Gregáň F, Holý A, Sigel H (1993) J Chem Soc Dalton Trans 1537–1546
62. Blindauer CA, Sigel A, Operschall BP, Holý A, Sigel H (2013) Z Anorg Allg Chem 639:1661–1673 (special issue on Bioinorganic Chemistry)
63. Bastian M, Chen D, Gregáň F, Liang G, Sigel H (1993) Z Naturforsch B 48:1279–1287
64. Gómez-Coca RB, Blindauer CA, Sigel A, Operschall BP, Holý A, Sigel H (2012) Chem Biodivers 9:2008–2034
65. Sigel H (1995) Coord Chem Rev 144:287–319
66. Gómez-Coca RB, Kapinos LE, Holý A, Vilaplana RA, González-Vilchez F, Sigel H (2000) Met Based Drugs 7:313–324 (Marc Leng memorial issue)
67. Davies DB, Rajani P, Sadikot H (1985) J Chem Soc Perkin Trans 2 279–285
68. Sigel H, Song B (1996) Met Ions Biol Syst 32:135–205
69. Aoki K, Murayama K (2012) Met Ions Life Sci 10:43–102
70. Blindauer CA, Holý A, Dvořáková H, Sigel H (1997) J Chem Soc Perkin Trans 2 2353–2363
71. Schwalbe CH, Thomson W, Freeman S (1991) J Chem Soc Perkin Trans 1 1348–1349
72. Massoud SS, Sigel H (1989) Inorg Chim Acta 159:243–252
73. Sigel H, Tribolet R (1990) J Inorg Biochem 40:163–179
74. Sigel H (1990) Coord Chem Rev 100:453–539
75. Sigel H, Hofstetter F, Martin RB, Milburn RM, Scheller-Krattiger V, Scheller KH (1984) J Am Chem Soc 106:7935–7946
76. Pelletier H, Sawaya MR, Kumar A, Wilson SH, Kraut J (1994) Science 264:1891–1903
77. Pelletier H (1994) Science 266:2025–2026
78. Pelletier H, Sawaya MR, Wolfle W, Wilson SH, Kraut J (1996) Biochemistry 35:12762–12777
79. Steitz TA (1999) J Biol Chem 274:17395–17398
80. Steitz TA (1998) Nature 391:231–232
81. Brautigam CA, Steitz TA (1998) Curr Opinion Struct Biol 8:54–63
82. Sigel H, Song B, Blindauer CA, Kapinos LE, Gregáň F, Prónayová N (1999) Chem Commun 743–744
83. Sigel H (1999) Pure Appl Chem 71:1727–1740
84. Sigel H (1992) Inorg Chim Acta 198–200:1–11
85. Freisinger E, Grollman AP, Miller H, Kisker C (2004) EMBO J 23:1494–1505
86. Tari LW, Matte A, Goldie H, Delbaere LTJ (1997) Nat Struct Biol 4:990–994
87. Robbins BL, Greenhaw J, Connelly MC, Fridland A (1995) Antimicrob Agents Chemother 39:2304–2308
88. Krejcova R, Horska K, Votruba I, Holý A (2000) Collect Czech Chem Commun 65:1653–1668
89. De Clecq E (1998) Collect Czech Chem Commun 63:449–479
90. De Clecq E (1998) Pure Appl Chem 70:567–577
91. Kramata P, Votruba I, Otová B, Holý A (1996) Mol Pharmacol 49:1005–1011
92. Birkuš G, Votruba I, Holý A, Otová B (1999) Biochem Pharmacol 58:487–492
93. Sigel H (2004) Pure Appl Chem 76:375–388
94. Sigel H, Da Costa CP, Song B, Carloni P, Gregáň F (1999) J Am Chem Soc 121:6248–6257
95. Song B, Zhao J, Gregáň F, Prónayová N, Sajadi SAA, Sigel H (1999) Met Based Drugs 6:321–328
96. Al-Sogair FM, Operschall BP, Sigel A, Sigel H, Schnabl J, Sigel RKO (2011) Chem Rev 111:4964–5003